

Monte Carlo studies on the sensitivity of the HEGRA imaging atmospheric Čerenkov telescope system in observations of extended γ -ray sources

A. Konopelko ^a, F. Lucarelli ^{a,b}, H. Lampeitl ^a and
W. Hofmann ^a

^a*Max-Planck-Institut für Kernphysik, D-69029 Heidelberg, Germany*

^b*Facultad de Ciencias Físicas, Universidad Complutense, E-28040 Madrid, Spain*

Abstract

In this paper, we present the results of Monte Carlo simulations of atmospheric showers induced by diffuse γ -rays as detected by the high-energy gamma-ray astronomy (HEGRA) system of five imaging atmospheric Čerenkov telescopes (IACTs). We have investigated the sensitivity of observations on extended γ -ray emission over the entire field of view of the instrument. We discuss a technique to search for extended γ -ray sources within the field of view of the instrument. We give estimates for HEGRA sensitivity of observations on extended TeV γ -ray sources.

PACS: 95.55.Ka; 95.55.Vj; 96.40.Pq

Keywords: Imaging atmospheric Čerenkov technique, very-high-energy gamma-ray astronomy

1 Introduction

During the last decade, very-high-energy (VHE) γ -ray astronomy ($E_\gamma > 100$ GeV), which utilizes ground-based imaging atmospheric Čerenkov telescopes (IACTs), has made a substantial contribution to the γ -ray astrophysics of a number of extra-galactic and galactic objects (for a review, see [1,2]). One of the reasons has been the tremendous progress in the observational technique. One can point out two major trends in this direction. The first is the use of imaging cameras with very fine pixellation (a pixel size of about 0.1°), equipped with fast electronics and an intelligent trigger, for a single stand-alone telescope, accomplished by Whipple [3], CAT [4] and CANGAROO [5]. Secondly, there

has been the development of the stereoscopic observational technique with a number of IACTs with imaging cameras of relatively coarse pixellation (a pixel size of 0.25°), primarily by the high-energy gamma-ray astronomy (HEGRA) collaboration [6]. Both trends have finally converged in three future experiments—H.E.S.S. [7], CANGAROO III [8] and VERITAS [9], which are the systems of a 10 m class of telescope. Another major project, called MAGIC [10], is a single telescope with a very large reflector of 17 m. Aspects of stereoscopic observations with three such telescopes have been discussed in [11].

For γ -ray point sources, the sensitivity of the imaging atmospheric Čerenkov technique substantially relies on the angular resolution of the instrument. Note that the methods of cosmic-ray rejection based on the analysis of image shape are still not effective enough to reduce entirely the background of hadronic air showers. Thus, in addition, a good angular resolution significantly reduces the background contamination induced by the isotropic cosmic rays.

The observations of γ -ray showers with a single telescope do not allow a complete geometrical reconstruction of the shower axis in space, because only one projection of a shower is available per event. A full reconstruction becomes possible in observations with two or more telescopes offering simultaneously a number of views of an individual shower. However, using advanced methods based on the strong correlation between the shape of the Čerenkov light images and their angular distances to the source position, one can achieve for a single IACT an angular resolution for an individual γ -ray shower of about 0.12° [12,13,14] using a fine pixellation camera.

A substantial improvement of the angular resolution has been achieved by the HEGRA collaboration using a stereoscopic system of five IACTs with rather coarse camera pixellation. The stereoscopic observations with such a system allow us to reach, with good quality data, an angular resolution for an individual γ -ray as good as 0.06° [15]. The rich HEGRA data sample of γ -rays from the Crab Nebula [16], Mkn 501 [17] and Mkn 421 [18] have allowed us to prove in great detail this angular resolution, which is in good agreement with the predictions based on the Monte Carlo simulations (for details, see [6]). Such an angular resolution has allowed us to perform a systematic search for point-like γ -ray sources at the flux level of 10^{-11} erg cm $^{-2}$ s $^{-1}$. Such high sensitivity was confirmed by the detection of a very faint γ -ray source, the supernova remnant (SNR) Cas A, which steadily emits γ -rays at the flux level of about 5.9×10^{-13} ph cm $^{-2}$ s $^{-1}$ above 1 TeV [19].

The HEGRA system of five IACTs has proved a very effective tool to search for TeV γ -ray emission and to study the energy spectra of point-like sources, which are well established in observations at other wavelengths. However, the potential γ -ray source may appear anywhere within the entire field of view (FoV) of the instrument, or it may have a rather large angular size as compared to the angular resolution of the instrument, for a certain number of important tasks, such as: (i) to search for γ -ray emitters with poorly known position (such as the EGRET unidentified sources); (ii) to perform sky surveys; (iii) to study extended γ -ray emission from supernova remnants; (iv) to investigate diffuse emission from the Galactic plane; and finally, (v) to detect the primordial γ -ray bursts. In

the following, we investigate the sensitivity in detecting γ -ray emission with the HEGRA system of IACTs in observations of this type. For this purpose, we have performed Monte Carlo simulations of diffuse γ -rays as well as isotropic cosmic rays (see sections 2 and 3). The simulations are compared with real data taken with the HEGRA system of IACTs (section 4). An important issue is the efficiency of applying the orientational and shape cuts in order to distinguish the γ -rays from the background isotropic cosmic rays. Here we study how this efficiency depends on the angular distance of a γ -ray source to the centre of the FoV (section 5). In section 6, we discuss the analysis techniques to search for point-like and extended γ -ray sources with the HEGRA system of IACTs, and finally in section 7 we give sensitivity estimates for shell-type supernova remnants.

2 Simulations

The simulations have been carried out using a two-step procedure, which has been described in detail in [6]. In the first step, the showers of primary γ -rays and protons were generated in the atmosphere using the ALTAI Monte Carlo code [20]. The showers were randomized over an impact distance with respect to the centre of the telescope array up to a maximum of 250 m. The major parameters of the samples of the simulated showers are summarized in table 1. The simulations have been carried out for different zenith angles, covering the range of angles usually used in observations of extended sources with the HEGRA system of IACTs. In the second step, the response of the telescope camera was simulated for all previously generated showers. This procedure accounts for all efficiencies of the Čerenkov light detectors (for details, see [21]). For the protons as well as for the γ -rays, an additional randomization of the images within a solid angle around the telescope axis with a half opening angle of 4.0° was introduced in order to simulate the isotropic flux of the proton showers and the diffuse γ -rays.

The simulations were carried out for the final HEGRA set-up of five IACTs¹. Each of the telescopes consists of an 8.5 m^2 reflector focusing the Čerenkov light on to a camera of 271 photo-multipliers arranged in a hexagonal matrix covering a FoV with an effective radius of 2.15° . The telescope camera triggers when the signal in two next-neighbours of the 271 photo-multiplier tubes exceeds a threshold of 8 mV ($\simeq 6$ photoelectrons), and the system readout starts when at least two telescopes are triggered by Čerenkov light from an atmospheric shower. The simulation procedure briefly described above was previously used for the production of the simulated data for the HEGRA system of IACTs [6]. Different parameters of the simulated cosmic-ray-induced as well as γ -ray-induced atmospheric showers have been compared to the data (see [6,22,23,24]).

¹ As the commissioning of the telescope system extended over several years, early data sets use three or four telescopes.

Table 1

Summary of the sample of Monte Carlo simulated showers.

Primary	Zenith angle ($^{\circ}$)	No of events	Energy (TeV)
γ	0	33239	0.1 - 30
	20	106810	0.4 - 30
	30	96729	0.4 - 30
	45	74641	0.4 - 30
p	0	21119	0.2 - 50
	20	30153	0.2 - 50
	30	41717	0.3 - 100
	45	29028	0.3 - 100

3 Analysis

The HEGRA system of IACTs is the first stereoscopic system to perform routine observations. Its basic idea is to observe atmospheric showers from a number of different viewing angles. The stereoscopic analysis of the system data is based on the geometrical reconstruction of the shower development in space, and consequently allows us to measure the arrival direction of each individual shower (for details, see [15]). By superposition of the several images in one common focal plane, one can determine the intersection point of the major axes of the ellipsoid-like images. This intersection point gives the direction of the shower. When the telescope system points directly towards the object, the reconstructed source position is in the centre of the FoV. However, in most observations of point-like γ -ray sources with the HEGRA system of IACTs, so-called ‘wobble mode’ observations have been made. In such a case, the position of the source is offset by 0.5° from the camera centre, allowing us to perform continuous ON-source observations with the corresponding OFF region taken at 1° offset from the source position across the camera centre.

In observations of extended γ -ray sources or diffuse γ -ray emission, one can divide the FoV into square bins of a size approximately equal to the angular resolution, accumulate ON-source and OFF-source events in these bins according to the reconstructed shower directions, and calculate the significance of a possible excess for each bin. Events are pre-selected according to their image shapes, to reduce the cosmic-ray background. Such an analysis is discussed below in detail. An alternative analysis technique is to use a grid which is much finer than the resolution, and to accumulate for each grid point the ON-source and OFF-source events with the directions consistent with a source localization at that point [25]. This technique is suitable to search for isolated point sources of an unknown location. But it has the disadvantage that the significances determined for adjacent grid points are highly correlated, which makes it difficult to judge the overall significance for an extended source.

In the case when an appropriate model of diffuse γ -ray emission can be easily constructed, one can use the likelihood ratio method to test the hypotheses (see section 7). If the expected emission region is relatively small, i.e. less than 0.5° in radius, in observations of such sources one can use a wobble mode approach by setting a corresponding offset of the target from the centre of the FoV, and by using the angular area symmetric across the centre of the FoV for the background estimate.

3.1 Detection rate

The counting rate of isotropically distributed cosmic rays and diffuse γ -rays after the application of shape cuts, $\tilde{R}_{(\gamma,cr)}$ [Hz str $^{-1}$], is defined as

$$\tilde{R}_{(\gamma,cr)}(\Theta) = R_{(\gamma,cr)}(\Theta)\eta_{(\gamma,cr)}(\Theta), \quad (1)$$

where $R_{(\gamma,cr)}$ is the counting rate of cosmic rays or γ -rays before the cuts, and $\eta_{(\gamma,cr)}$ is the acceptance after applying the shape cuts. Θ is the angular distance from the centre of the FoV. The initial event counting rate $R_{(\gamma,cr)}$ can be calculated as

$$R_{(\gamma,cr)}(\Theta) = N_{(\gamma,cr)}\Delta t^{-1}\Delta\Omega^{-1}, \quad (2)$$

where $N_{(\gamma,cr)}$ is a number of registered events during the time interval Δt within the solid angle $\Delta\Omega$, which is usually chosen to reflect the angular resolution of the instrument. In calculations we used the cosmic-ray energy spectra given in [26].

For diffuse and extended γ -ray sources there is no direct correlation between the impact distance of a shower (the distance of the shower axis to the geometrical centre of the array) and the location of the image centroid position in the FoV. Showers detected at the same impact distance but of different inclinations with respect to the telescope axis could produce an image positioned anywhere in the FoV, which is limited by the angular size of the telescope imaging camera.

The calculated γ -ray detection rate, R_γ , as a function of the angular distance from the telescope axis is shown in figure 1 for different trigger multiplicities (the number of triggered system telescopes). One finds a constant detection rate up to $\Theta = 1^\circ$ (within 10%) from the centre of the FoV and a rather sharp decrease beyond that region. For the higher trigger multiplicities, the fall-off in the detection rate starts at smaller angular distance from the telescope axis. This rather sharp decrease can be explained as follows. In a toy model one can assume that most of the detected γ -ray showers have an impact distance around $R_o \simeq 120$ m (see, for example, [27]). The γ -ray-induced atmospheric showers, which have a primary energy above the energy threshold of the instrument ($E > 500$ GeV), and which have shower axes directed along the joint optical axis of the system telescopes, will produce the Čerenkov light images with the centroid positions shifted from the camera

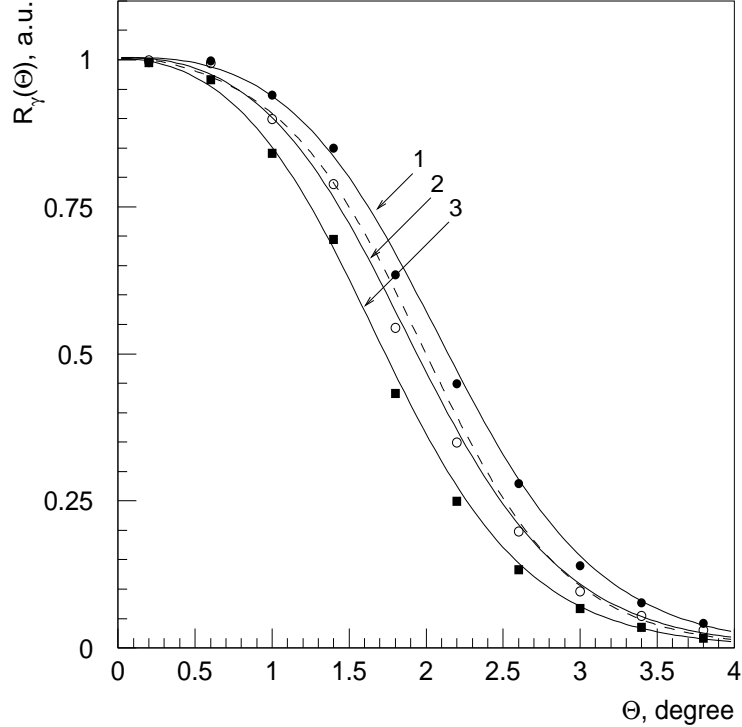


Fig. 1. Detection rate of the isotropically distributed γ -rays and cosmic rays calculated for the HEGRA system of IACTs. The solid curves represent the γ -rays. Curves 1, 2 and 3 correspond to the trigger multiplicities of 2, 3 and 4, respectively. The symbols correspond to the Monte Carlo data points used in the fits. The dashed curve shows the rate of the cosmic-ray showers for the trigger multiplicity of 2. Detection rates are normalized to 1 at the centre of the FoV. The rates were calculated after applying the quality cuts, distance $< 1.8^\circ$, and image size > 40 photoelectrons. Hereafter, a.u. as indicated along the Y-axis denotes arbitrary units.

centre by approximately $\Theta_o \simeq 1^\circ$. These images are well within the effective radius of the HEGRA cameras of 2.15° . Diffuse γ -rays, coming at the inclination angle of about $\Theta_s \geq 1.1^\circ$ with respect to the telescope axis, will often be truncated by the camera edge (see figure 2), and the acceptance of these showers will be substantially lower due to this effect. From such a toy model, one can expect a rather stable γ -ray rate, $R_{(\gamma,cr)}(\Theta)$, up to $\Theta \simeq 1.1^\circ$. Note that, by increasing the energy of the detected γ -ray showers, the effective impact distance increases as well and consequently this effect of the camera edge shows up at smaller shower inclinations.

The detection rate as a function of the angular distance from the centre of the FoV can be well fitted as

$$R_{(\gamma,cr)}(\Theta) = a_0 \cdot (1 + \Theta)^{a_1} [1 + \exp(a_2 \cdot (\Theta - a_3))]^{-1}. \quad (3)$$

The parameters of the fit are given in table 2 for the γ -ray-induced and cosmic-ray-induced showers (see figure 1).

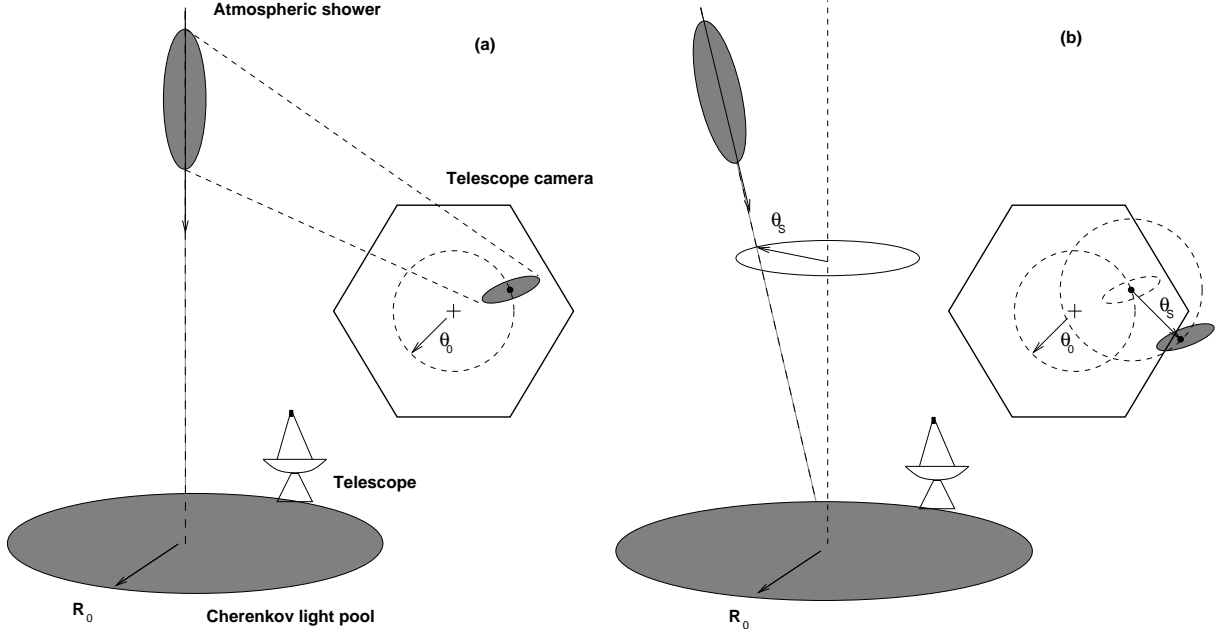


Fig. 2. Schematic diagram of the image displacement in the camera focal plane.

Table 2

Parameters of the fit (equation (3)) for the simulated diffuse γ -ray-induced and cosmic-ray-induced atmospheric showers, registered with the HEGRA system of IACTs.

	No of telescopes	a_0	a_1	a_2	a_3
γ	2	1.021	0.060	1.905	2.052
	3	1.032	0.065	1.932	1.840
	4	1.042	0.070	1.985	1.624
cr	2	1.010	0.060	2.316	1.824
	3	1.035	0.065	2.261	1.507
	4	1.060	0.075	2.406	1.174

3.2 Angular resolution

The angular resolution of the IACT array heavily relies on the accuracy of the reconstruction of the image major axis, which in turn depends mainly on the image size and the distance of the shower axis to the centre of the array (impact distance). The images taken at relatively large impact distances have an elongated angular shape and offer an accurate determination of the image orientation. Note that at very large impact distances (only for a central point source) the images can be truncated by the camera edge. These images may distort the reconstruction, but they can be removed from the analysis by using the cut on angular distance of the image centre of gravity (centroid) to the camera centre (here we use a cut on distance $< 1.8^\circ$). Thus, images with a rather large number

of photoelectrons (well above 40), and which are detected at impact distances within the range of 50–200 m, offer the best determination of the direction of the arriving shower [6]. This explains why, with the increase in primary energy of the shower, the angular resolution improves so much (for detailed discussions, see [6,15]).

Finally, the angular resolution of the IACT array strongly depends on the multiplicity of the system trigger [6]. The analysis of the HEGRA Mkn 501 data sample [15] has shown that using three images out of four allows us to achieve an angular resolution which is by roughly two times better than the resolution achieved when using two images. At the same time, the use of higher trigger multiplicities leads to a slightly higher energy threshold of the instrument. All this may constrain the choice of the optimum analysis scheme.

The angular resolution for a γ -ray source placed at a different angular distance from the centre of the FoV is illustrated in figure 3 and table 3. One can see that the geometrical reconstruction of the direction of the arriving shower also works very well for slightly inclined γ -ray showers, and the angular resolution almost does not depend on the angle Θ within the range of $\Theta \leq 1.5^\circ$. However, beyond this region the images detected with the telescope system are often truncated by the camera edge, which worsens the angular reconstruction. For the precise measurements of an angular extension of a γ -ray source one should take into account the actual angular resolution at a certain angular distance from the centre of the FoV, and perform the deconvolution to obtain the measured angular extension of the source.

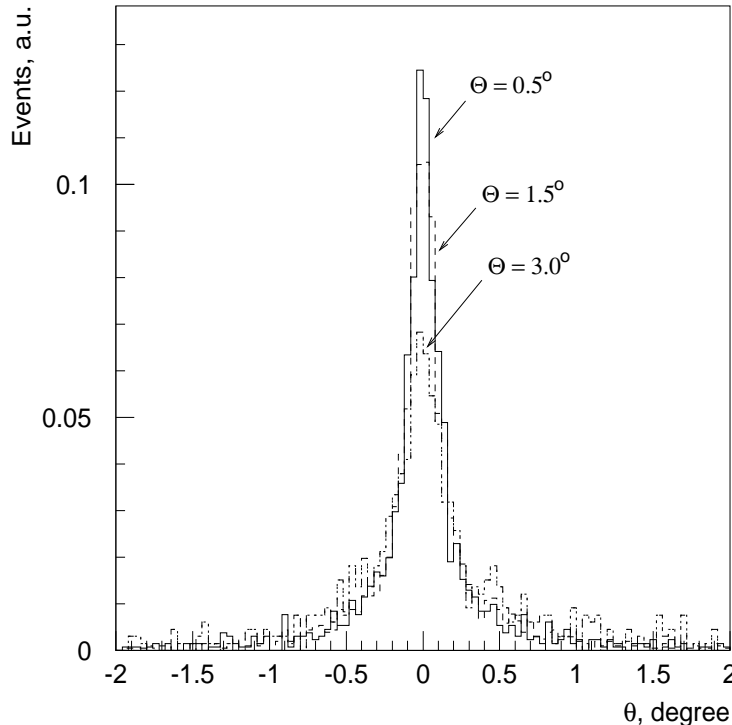


Fig. 3. The angular resolution of the OFF-axis γ -ray showers detected with the HEGRA system of IACTs. At least three images were used for the reconstruction of the direction of the arriving shower.

Table 3

Angular resolution for an individual off-axis γ -ray-induced atmospheric shower ($\Delta\theta$ defines a 68% error circle around an actual source position).

Θ ($^\circ$)	0.5	1.0	1.5	2.0	2.5	3.0
$\Delta\theta$ ($^\circ$)	0.12	0.12	0.14	0.16	0.17	0.31

Table 4

Acceptances of γ -ray-induced and cosmic-ray-induced atmospheric showers after the analysis by a mean scaled width cut of 1.1.

Trigger	Θ ($^\circ$)	0.5	1.0	1.5	2.0	2.5	3.0
2/5	k_γ	0.67	0.68	0.69	0.62	0.58	0.41
3/5	k_γ	0.66	0.67	0.68	0.62	0.55	0.34
4/5	k_γ	0.65	0.65	0.66	0.60	0.50	0.21
2/5	k_{CR}	0.06	0.06	0.06	0.06	0.07	0.08
3/5	k_{CR}	0.04	0.04	0.04	0.04	0.05	0.07
4/5	k_{CR}	0.03	0.03	0.03	0.04	0.06	0.08

3.3 Rejection of cosmic rays

Apart from the excellent angular resolution, the IACT system offers the ability to reject cosmic-ray showers using the shape of the Čerenkov light images registered in a number of telescopes. Imaging cameras detect, in addition to the Čerenkov light from the atmospheric showers, all kinds of background light (e.g. night sky background light, direct star light, etc). To remove most of the camera pixels containing exclusively the background light, a specific image clearing procedure is usually applied. The pixels with light intensity below some fixed intensity limit are sorted out of the image. The images of the high-energy γ -ray showers detected close to the telescope system embrace many more pixels as compared to low-energy events or to the same event but at rather large impact distance. Using the standard second moment analysis, one can obtain very different angular sizes of recorded images, depending on the primary shower energy and shower impact distance.

In order to avoid the dependence of an image on the shower energy and impact distance, one can derive using the standard image parameter width, the parameter mean scaled width, $\langle\tilde{w}\rangle$ [28,29] for each individual event:

$$\langle\tilde{w}\rangle = 1/n \sum_{k=1}^n w_k / \langle w \rangle_k^{ij}. \quad (4)$$

Here n is the number of triggered telescopes, w_k is the width for the k th image and $\langle w \rangle_k^{ij}$ is the expected mean image width calculated beforehand from the Monte Carlo simulations over a number of bins on the impact distance ($\Delta r_i, i = 1, n$) and image size

$(\Delta \log(S_j), j = 1, m)$ [6]. The mean scaled width parameter has been proven to be an effective tool in rejection of a substantial fraction of the cosmic-ray showers. For central point-like γ -ray sources, applying a cut on mean scaled width of $\langle \tilde{w} \rangle < 1.1$ provides for the system trigger 4/4 an acceptance of γ -rays at 65%, whereas the cosmic-ray contamination is reduced by this cut by a factor of 30, corresponding to an enhancement of the γ -ray sample (Q-factor = $k_\gamma k_{CR}^{-1/2}$) of 3.7.

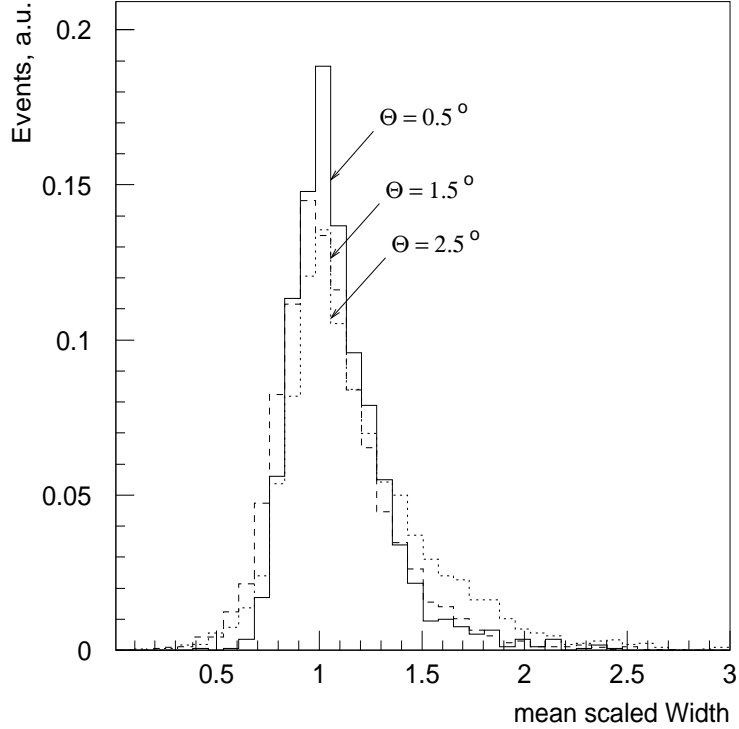


Fig. 4. *The distribution of the mean scaled width parameter for the samples of γ -rays at three inclination angles with respect to the telescope optical axis. Events with at least two images were used in the analysis.*

Here we study how the cut on mean scaled width works for the γ -rays coming off the telescope optical axis. The calculations have been made for six bands, each of a size of 0.2° , centred at the angular distances of 0.5° , 1° , 1.5° , 2.0° , 2.5° and 3.0° , from the centre of the FoV. The distributions of the mean scaled width for the γ -ray showers within three of these bands are compared in figure 4. With an increasing angle relative to the axis, the distributions remain peaked at 1, but develop a tail towards larger $\langle \tilde{w} \rangle$. The acceptances of the γ -rays after applying the cut on mean scaled width are almost identical for these bands. We may conclude that the shape of the images for the γ -ray showers coming off the telescope optical axis at angles less than $\simeq 1.5^\circ$ are still not noticeably affected by the telescope camera edge. One can see a slight decrease in the γ -ray acceptance, k_γ , towards larger displacements from the centre of the FoV, which is related to the effect of the camera edge. For the isotropically distributed cosmic rays, the acceptance after applying the mean scaled width cut (k_{cr}) also does not depend on the angular distance within the range of $\Theta \leq 2^\circ$ (see table 4), whereas it increases slightly towards larger

Table 5

The calculated and measured detection rate, R_γ , hr^{-1} , of the Crab Nebula at 0.5° distance from the centre of the FoV.

Trigger	2/4	3/4	4/4
Data	18 ± 2	21 ± 3	19 ± 3
Monte Carlo	20	20	22

angular distances.

4 Simulations versus data

The simulations of the diffuse γ -rays can be verified by the observations of the Crab Nebula. The observations in the wobble mode correspond to the angular displacement of the source by 0.5° from the centre of the FoV. Assuming in the simulations the Crab Nebula flux and spectrum as measured by the HEGRA collaboration [16], one can calculate the corresponding γ -ray rate at the same angular distance from the centre of the FoV. The results for different trigger multiplicities are summarized in table 5. The Monte Carlo simulations reproduce well the relative rates for two, three and four telescopes. Note that the possible systematic error of the Monte Carlo simulated rates is estimated to be less than 10%.

The distributions of the mean scaled width parameter for the γ -ray-induced and cosmic-ray-induced showers are shown in figure 5. The Monte Carlo distributions fit very well with the data. Here, the same Monte Carlo tables of mean width as function of impact distance and image size have been used for the simulated and recorded events. For each individual event, the Monte Carlo tables were interpolated according to the reconstructed impact parameter and measured image size in simulations and in the data. Simulations are in very good agreement with the data. The position of the peak of the simulated γ -ray showers agrees within 3% with the data. The data distribution of the γ -rays was produced using the HEGRA Crab Nebula data sample [16].

5 Sensitivity over FoV

The sensitivity of the HEGRA system over the whole FoV can be estimated using the detection rates and acceptances previously discussed. To parametrize the sensitivity of the instrument one can use the Q -parameter calculated as

$$Q(\Theta) = k_\gamma R_\gamma \cdot [k_{CR} R_{CR}]^{-1/2} \tag{5}$$

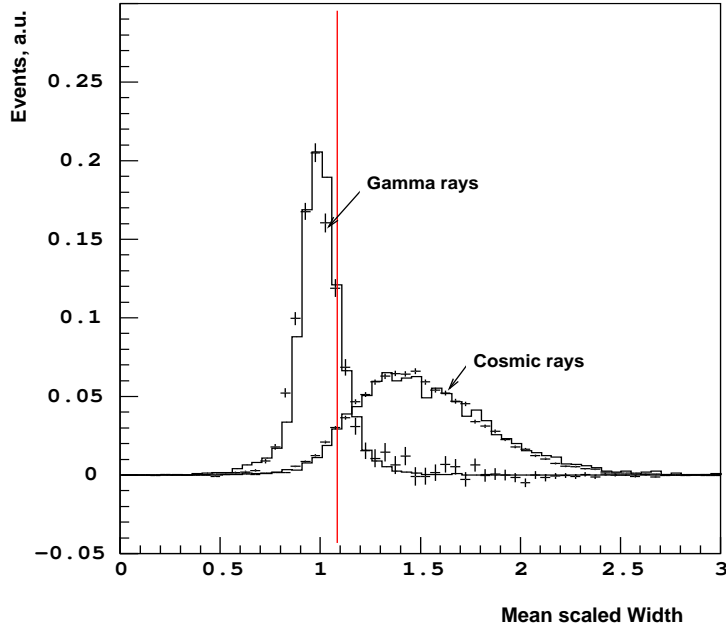


Fig. 5. The distributions of the mean scaled width parameter for the sample of γ -rays and cosmic rays. Histograms show the Monte Carlo simulations. The crosses denote the HEGRA data taken with the system trigger as two telescopes out of five. The distributions are normalized to one particle. The content of the histogram bins is given in arbitrary units.

where the rates of the γ -rays and cosmic rays are normalized to 1 at $\Theta = 0$. The results of such calculations are shown in figure 6. One can see that the value of the Q -parameter is constant up to $\Theta = 1^\circ$. Even though the γ -ray detection rate decreases noticeably beyond that region the Q -parameter at $\Theta = 1.5^\circ$ is only 5% less than in the central part of the FoV.

The higher telescope multiplicities provide a better Q -factor. This is due to the fact that for higher multiplicities the cosmic-ray rejection is substantially better, even though the detection rate of the γ -rays decreases at larger angular distances from the centre of the camera. The sharp decrease in γ -ray rate at large angular distances ($\Theta \geq 2.5^\circ$) finally makes observations with higher telescope multiplicities less effective.

Note that the angular resolution is almost constant up to the angular distance of 1° .

In observations of the Crab Nebula with the HEGRA system of IACTs at zenith angles $\leq 35^\circ$, the numbers of γ -ray and cosmic-ray showers detected in one angular bin ($\Delta\Omega \simeq 5 \times 10^{-5}$ str), placed at the centre of the camera, in one hour (before applying the shape cuts) are about 80 and 406 (counts hr^{-1}), respectively. These measured rates can be reproduced with high accuracy using the Crab Nebula spectrum as measured by HEGRA [16], and using the fluxes and spectra of cosmic rays given in [26]. One can calculate the signal-to-noise ratio after 1 h observations as $S/N = (ON - OFF)/(ON + OFF)^{1/2} = N_\gamma / [(N_\gamma + N_{\text{cr}}) + N_{\text{cr}}]^{-1/2} \cdot Q(\Theta)$. Thus, in the centre of the FoV the signal-to-noise ratio is $S/N \simeq 7.5\sigma \text{ hr}^{-1}$ for the trigger multiplicity 2/5, which agrees with the value directly measured

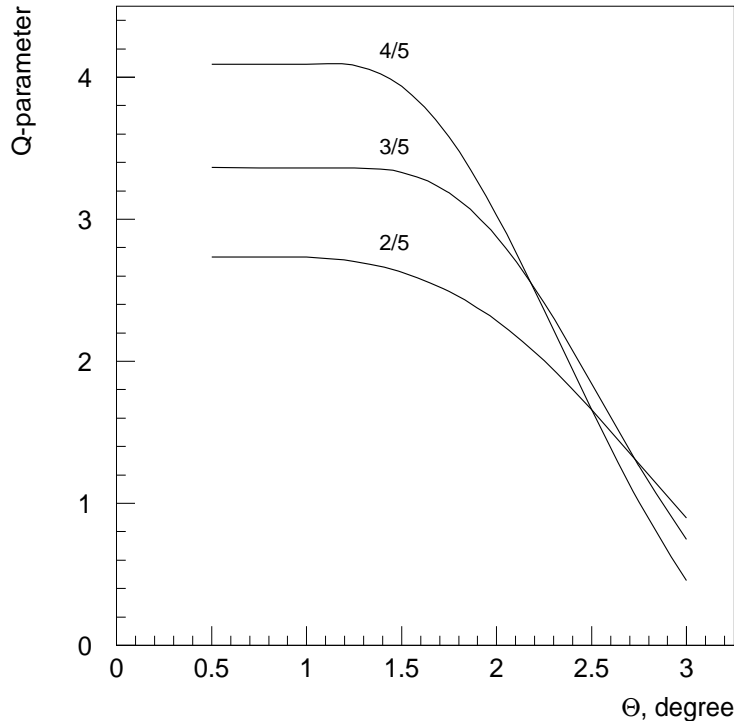


Fig. 6. Q -factor (equation (5)) calculated at different angular distances from the centre of the FoV. Corresponding trigger multiplicities are shown.

in observations of Crab Nebula ($S/N \simeq 7.6\sigma \text{ hr}^{-1}$). One can obtain an improvement by a factor of 1.25 and 1.5 for the multiplicities of $3/5$ and $4/5$, respectively, on the Crab Nebula data sample as well as for the simulated data.

6 Estimate of the significance of excess

In observations of extended γ -ray sources or diffuse γ -ray emission from certain regions of the sky, it is not trivial to calculate properly the significance of a possible excess of the γ -ray candidates. In order to calculate this significance, one could follow different procedures, depending on whether the OFF-runs (data taken out of the source direction) are available or not. However, in both cases it is necessary to calculate the detection efficiency versus the radial distance from the centre of the FoV directly from the data and, afterwards, to apply a flat fielding in order to compensate for the non-uniform response of the camera at different angular distances. One can fit the detection rate of the cosmic rays versus the angular shift from the centre of the FoV and then apply that fit to all angular bins over the entire FoV. Such a fit can vary accordingly to the source zenith angle and the night sky background, and can also have an azimuthal dependency. However, our studies of the azimuth dependence did not reveal a significant effect for the rather symmetric HEGRA system of IACTs.

Since the stereoscopic reconstruction of atmospheric showers with the HEGRA system of

IACTs allows us to calculate the right ascension (RA) and declination (DEC) for each individual event as well as the angular slopes of the shower axis in the joint focal plane, it is possible to produce a two-dimensional map of the reconstructed events over the FoV, after applying the standard cut on mean scaled width, e.g. $\langle \tilde{w} \rangle < 1.1$, in order to separate γ -rays from hadrons. The observational window can be divided into square cells of size $0.2^\circ \times 0.2^\circ$, which is close to the optimum, given the angular resolution of the HEGRA system of IACTs ($\text{RMS} \simeq 0.1^\circ$). At the same time such bin size allows us to have a relatively large number of pixels for computing the average number of cosmic-ray hits per angular bin, which can be used to estimate the average background content per angular bin. As noted in section 3, the region of almost constant sensitivity is limited by roughly 1° from the centre of the FoV. Given the number of counts for each bin, one can calculate the significance for each bin, S , using the corresponding OFF data sample.

Let us now examine two cases separately. If both ON-source and OFF-source data are available, after applying the mean scaled width cut the mean number of counts per angular bin in ON-source and OFF-source data samples can be calculated as

$$\langle N_{(on,off)} \rangle = \frac{1}{M} \sum_{i=1}^M N_{(on,off)}(i, \Theta) f^{-1}(\Theta) \quad (6)$$

where $N_{(on,off)}(i, \Theta)$ is the number of counts in i th bin at a certain distance, Θ , from the centre of the FoV. Function $f(\Theta)$ accounts for the non-constant event rate at different radial distances. M is the total number of bins in the grid. $\langle N_{off} \rangle$ is the mean number of counts per bin placed at the centre of the camera's FoV in the OFF-source sample. Given this number, one can estimate the background content for each camera pixel (i) for ON-source data as

$$N_{off}^{(1)}(i) = \alpha f(\Theta) \langle N_{off} \rangle \quad (7)$$

The scaling factor α can be determined as

$$\alpha = \langle N_{on} \rangle (\langle N_{off} \rangle)^{-1}, \quad (8)$$

which equalizes the difference in observational time for ON-source and OFF-source samples, as well as possible differences in corresponding zenith angle distributions.

In the case when only ON-source data are available, one can use a mean number of counts per bin² averaged over all bins in the ON-source data sample, $\langle N_{on} \rangle$. It is assumed here

² Note that in observations of extended γ -ray sources with well-defined location and extension one can exclude from the averaging loop (equation (6)) the angular bins, which are *a priori* covered by the source. However, the source extension has to be significantly smaller than the observational window used.

that the expected rate of the γ -rays is very low and is negligible compared with the cosmic-ray rate.

Thus, the mean number of predicted background counts in each angular bin is given by

$$N_{off}^{(2)}(i) = \alpha f(\Theta) \langle N_{on} \rangle. \quad (9)$$

Here the scaling factor α is calculated as $\alpha \simeq 1/M$, where M is a total number of bins used in equation (6).

Finally, the significance for each individual angular bin can be estimated using the approach suggested in [30]. Assuming that the bins with high signal-to-noise ratio ($\simeq 3.5\sigma$) contain an excess of γ -rays one can exclude these pixels from calculating the average number of background counts per bin and recalculate the significances again. Such an iterative procedure can be repeated a number of times before the values of the significances finally converge.

The background model constructed from the ON-source data itself cannot be applied for observations of a presumably diffuse γ -ray source of a large angular size, which is comparable with the angular size of the entire FoV of the instrument. However it might be effective in a discovery mode while scanning very extended sky regions.

For a positive detection of a quite extended γ -ray source (with a size larger than 0.5°), one can expect that a few contiguous pixels should show a high value of significance. One can calculate the confidence level of the excess using the approach suggested by Li and Ma [30] for such a particular case. This approach takes into account that the confidence level of an excess in each bin depends, in addition, on the total number of bins (number of trials) M , which may be considered as M independent measurements.

After the average background calculation, we can calculate the standard deviation for each pixel from the average background. Naturally, only those pixels which show an excess in the ON data sample, (for instance, with $S > 3.5\sigma$, where σ is one standard deviation for the Gaussian distributed background events), might be considered for statistical analysis. The probability p to achieve 3.5σ excess due to fluctuations in background for each individual pixel, can be simply calculated as

$$p = 1 - \frac{1}{\sqrt{2\pi}} \int_{-\infty}^{3.5} e^{-\frac{1}{2}t^2} dt. \quad (10)$$

Eventually, the probability to obtain k pixels within our FoV will be given by

$$p_k = C_M^k p^k (1-p)^{M-k} \quad (11)$$

(C_M^k is the binomial coefficient). The results of calculations for different pixel multiplicities

Table 6

Estimates of the confidence level for the excess events. k is the number of pixels showing a 3.5σ excess from the average background.

k	p_k Eqn.(11)	p_k MC
1	$1.83 \cdot 10^{-2}$	$1.83 \cdot 10^{-2}$
2	$1.68 \cdot 10^{-4}$	$1.70 \cdot 10^{-4}$
3	$1.02 \cdot 10^{-6}$	$9.60 \cdot 10^{-7}$
4	$4.55 \cdot 10^{-9}$	$4.70 \cdot 10^{-9}$

in excess and $M = 80$ using equation (11) are provided in table 6. The calculations show, for example, that a four-pixel coincidence within the observational window composed of 80 pixels is an extremely rare case with a probability less than 10^{-8} and the corresponding estimate of confidence at 6σ level. But, in practice, one could observe one, two, three or even many more bins with a significant excess in the event rate. All these cases should be statistically tested taking into account the total number of selected angular bins within the FoV, which corresponds to the number of independent trials.

In order to prove the formulae given by equation (11), we have also made straightforward Monte Carlo simulations, randomizing the number of entries for $M = 80$ pixels according to a Gaussian distribution with average value $\langle N_{ON}(i) \rangle = 300$. The results are summarized in table 6 (see column p_k MC). One can see a rather good agreement between the direct Monte Carlo simulations and the values obtained from equation (11), taking into account a limited statistics in the Monte Carlo simulations which finally limits the accuracy of the calculations.

An alternative approach to estimate the significance for extended sources would be to make some assumptions about the position and the extension of the γ -ray source, based on physical arguments, taking as ON, the correspondent sky region, and as OFF, several sky regions of the same shape (if possible). One can calculate the corresponding significance using the approach of Li and Ma [30].

7 Sensitivity to extended γ -ray sources

TeV γ -ray emission, resulting from the π^0 -decay produced in nearby supernova remnants (SNR) by the accelerated protons colliding with the ambient thermal gas nuclei, is marginally high enough to be detectable by currently operating imaging atmospheric Čerenkov telescopes (see, for example, [31,32]). Given the angular size of the shell-type SNRs, which has been measured in radio wavelength range, the emission region in TeV γ -rays is expected to be significantly extended [32]. In good approximation, the source is characterized by the constant brightness in γ -rays all over the SNR radio extent.

Based on the detailed Monte Carlo simulations for the HEGRA system we have estimated

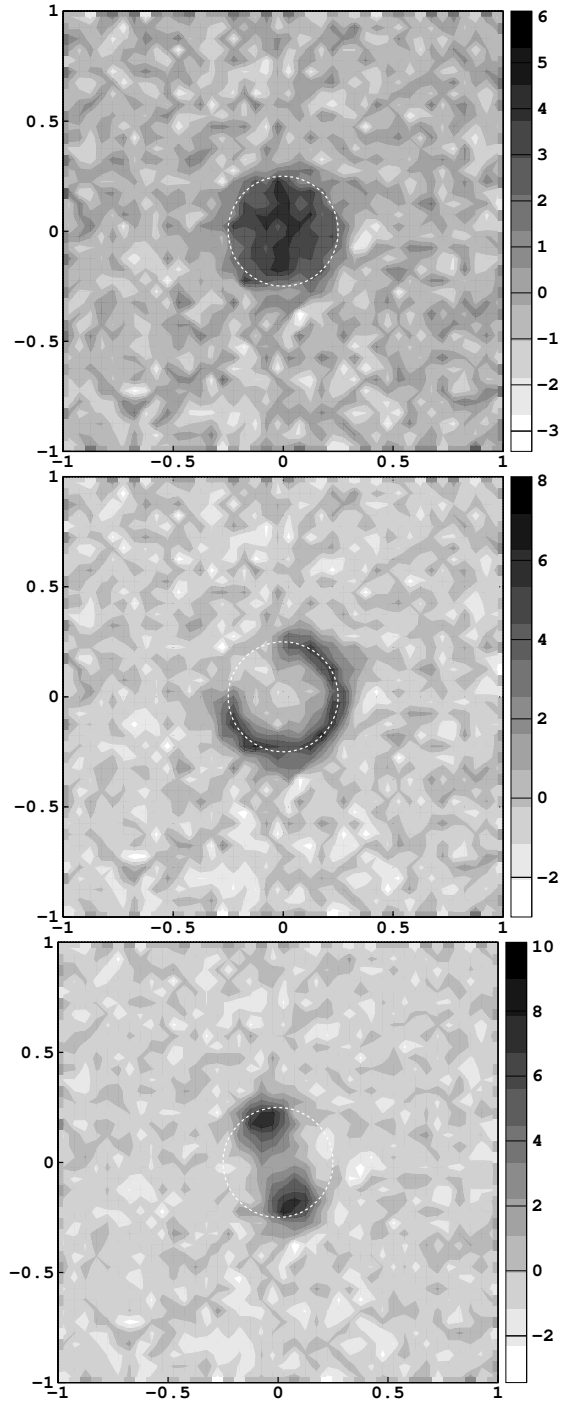


Fig. 7. Monte Carlo simulated response of the HEGRA system of five IACTs (Trigger: 2/5) after 100 h of observations of shell-type SNRs for three models of TeV γ -ray emission: ‘circle’ (upper panel); ‘ring’ model for the γ -rays simulated over 75% of the entire ring (central panel); ‘double-pole’ model (lower panel). For details on radial profiles of TeV γ -ray emission see [32]. The angular size of the SNR in radio wavelength is indicated by the dashed circle.

the sensitivity of the instrument in observations of extended γ -ray sources. The results of the simulations can be interpreted using the established sensitivity for a point-like γ -ray source. Thus, the resulting signal-to-noise ratio for a γ -ray source of an arbitrary angular size, θ , can be calculated as

$$S/N = \tilde{R}_\gamma / [\tilde{R}_{CR} \cdot (\theta/\theta_0)^2]^{1/2} t^{1/2} = \tilde{R}_\gamma / [\tilde{R}_{CR}]^{1/2} \cdot (\theta/\theta_0)^{-1} t^{1/2} \quad (12)$$

where \tilde{R}_γ and \tilde{R}_{CR} are the detection rates of γ -rays and cosmic rays, respectively, after applying the analysis cut. Values θ_0 and θ correspond to the orientational cuts for a point-like source ($\theta_0 = 0.1$) and extended γ -ray source (θ is a source extension). \tilde{R}_{CR} is a cosmic-ray rate for a standard orientational cut applied for a point source search. For the isotropic cosmic-ray background, the total number of background counts for an extended γ -ray source is proportional to the angular area covered by this source ($R_{CR} \propto \theta^2$). For a 5σ detection and fixed observational time³ ($t = 100$ h) one can calculate the minimum detectable flux from the point-like γ -ray source. For the HEGRA array of five IACTs such a minimum detectable flux is $F_\gamma^{p.s.} (\geq 1 \text{ TeV}) = 1.1 \cdot 10^{-12}$ photon $\text{cm}^{-2} \text{ s}^{-1}$. Finally, the minimum detectable flux for an extended γ -ray source is given by

$$F_\gamma^{ex.s.} = F_\gamma^{p.s.} \cdot (\theta/0.1 \text{ deg}), \quad (13)$$

where θ is an angular radius of a source region. Note that for an extended γ -ray source of large extension ($\theta > 0.5$ degree) the integral rates \tilde{R}_γ and \tilde{R}_{CR} need to be corrected for the fall-off in the camera response function (see figure 1). For γ -ray sources of large extension ($\theta > 1$ degree) one has to perform observations preferably in ON/OFF mode, i.e. taking the same amount of OFF data as for the ON data sample, because almost the entire sensitive area is covered by a source region. The results of the detailed Monte Carlo simulations may deviate from the estimates given by equation (13) for the γ -ray sources of angular extension substantially larger than 1° .

As an example, we consider here a shell-type SNR with an angular size of 0.25° (such as SN 1006). Three different models of TeV γ -ray emission have been discussed in [32]. The profiles of γ -ray brightness are taken from [32]. The leptonic model of γ -ray emission yields the uniform distribution of emitted γ -rays ('circle' model), whereas for hadronic models the brightness might peak around the shock front ('ring' model) or concentrate around two emission poles ('double-pole' model) [32] (see figure 7). We have modelled the response of the HEGRA system of five IACTs for the fluxes and brightness profile given in [32] after 100 h of observations (see figure 7) assuming the γ -ray flux given in [33]. The minimal observing time for a 5σ detection depends on the assumed morphology of the γ -ray emission. Thus, for the 'circle', 'ring' and 'double-pole' models the minimal detection times are 16 h, 5 h and 2 h, respectively. Deep observation of such an SNR could allow us to study in detail the morphology of the TeV γ -ray emission and finally to distinguish between different models of γ -ray emission.

³ For instance, SNR Cas A was observed with HEGRA system of IACTs for a total exposure time of 250 h [19].

8 Conclusion

The response of the HEGRA system of IACTs to the diffuse and extended γ -ray emission over the FoV of the instrument was studied by means of detailed Monte Carlo simulations. Within the angular region limited by 1° from the centre of the FoV the detection rate of the γ -rays as well as the quality factor, characterizing the efficacy of the γ -ray selection, are constant. Further extension of the observational window up to 1.5° still allows us to have the same sensitivity to the γ -ray fluxes but with noticeably reduced γ -ray detection rate. An analysis of different trigger multiplicities reveals an improvement in the sensitivity, whereas higher multiplicities lead to the substantial decrease in the γ -ray detection rate.

We have modelled the response of the HEGRA system of five IACTs for observations of nearby SNRs. Even though the final sensitivity estimate depends on the actual morphology of the TeV γ -ray emitting region, in a simple case of a ‘circular’ emission region the sensitivity might be derived by rescaling the sensitivity for a point-like source.

The studies discussed here could have a general use for the forthcoming arrays of IACTs such as CANGAROO, H.E.S.S. and VERITAS.

Acknowledgments. This work was supported by CICYT (Spain) and BMBF (Germany).

References

- [1] Ong, R. *Phys. Rep.*, 305, 93 (1998)
- [2] Catanese, M., Weekes, T.C. *PASP*, vol. 111, N 764, 1193 (1999)
- [3] Finley, et al. *Proc. ICRC*, 2001, Hamburg, vol.7, 2827 (2001)
- [4] Barrau, A., et al. *Nucl. Instrum. Methods A* 416, 278 (1998)
- [5] Kawachi, A. et al. *Astropart. Phys.*, 14,261 (2001)
- [6] Konopelko, A., et al. *Astropart. Phys.*, 10, 275 (1999)
- [7] Hofmann, W., et al. *Proc. 27th ICRC*, Hamburg, Germany, vol.7, 2785 (2001)
- [8] Mori, M., et al. *Proc. 27th ICRC*, Hamburg, Germany, vol.7, 2831 (2001)
- [9] Quinn, J., et al. *Proc. 27th ICRC*, Hamburg, Germany, vol.7, 2781 (2001)
- [10] Lorentz, E., et al. *Proc. 27th ICRC*, Hamburg, Germany, vol.7, 2789 (2001)
- [11] Magnussen, N., Meyer, H. *Proc. Workshop "Towards a Major Atmospheric Čerenkov Detector - V"*, Kruger National Park, South Africa, August 1997, 392 (1997)
- [12] Ulrich, M., Daum, A., Hermann, G., Hofmann, W. *J. Phys. G: Nucl. Part. Phys.*, 24, 883 (1998)
- [13] Le Bohec, S., et al. *Nucl. Instrum. Methods A* 416, 425 (1998)
- [14] Lessard, R., et al. *Astropart. Phys.*, 15, 1 (2001)
- [15] Hofmann, W., et al. *Astropart. Phys.*, 12, 135 (1999)
- [16] Aharonian, F., et al. *Astrophys. J.*, 539, 317 (2000)
- [17] Aharonian, F., et al. *Astron. Astrophys.*, 349, 11 (1999)
- [18] Aharonian, F., et al. *Astron. Astrophys.*, 350, 757 (1999)
- [19] Aharonian, F., et al. *Astron. Astrophys.*, 370, 112 (2001)
- [20] Konopelko, A., Plyasheshnikov, A. *Nucl. Instrum. Methods A* 450, 419 (2000)
- [21] Hemberger, M. PhD thesis, MPIH-V19-98 (1998)
- [22] Aharonian, F., et al. *Phys. Rev. D* 59, 092003 (1999)
- [23] Aharonian, F., et al. *Astron. Astrophys.*, 361, 1073 (2000)
- [24] Aharonian, F., et al. *Astropart. Phys.*, 10, 1 (1999)
- [25] Aharonian, F., et al. *Astron. Astrophys.*, 375, 1008 (2001)
- [26] Wiebel, B. *Univ. Wuppertal, Preprint WUB-94-08* (1994)

- [27] Aharonian, F., et al. *Astropart. Phys.*, 6, 343 (1997)
- [28] Konopelko, A. in: *Proc. Towards a Major Atmospheric Čerenkov Detector-IV*, Padova, ed. M. Cresti, 373 (1995)
- [29] Hofmann, W. in: *Proc. Towards a Major Atmospheric Čerenkov Detector-V*, Kruger Park, South Africa, ed. Okkie de Jager, 284 (1997)
- [30] Li, T. Ma, Y. *Astrophys. J.*, 272, 317 (1983)
- [31] Berezhko, E.G., Völk, H.J. *Astropart. Phys.*, 7 (1997)
- [32] Berezhko, E.G., Ksenofontov, L.T., Völk, H.J. *Astron. Astrophys.*, at press (2002); astro-ph/0204085
- [33] Tanimori, T., et al. *Astrophys. J.*, 497, L25 (1998)